One or Two Frequencies? The Empirical Mode Decomposition Answers

Gabriel Rilling and Patrick Flandrin, *Fellow, IEEE*

***Abstract*—This paper investigates how the *empirical mode decomposition* (EMD), a fully data-driven technique recently introduced for decomposing any oscillatory waveform into zero-mean components, behaves in the case of a composite two-tones signal. Essentially two regimes are shown to exist, depending on whether the amplitude ratio of the tones is greater or smaller than unity, and the corresponding resolution properties of the EMD turn out to be in good agreement with intuition and physical interpretation. A refined analysis is provided for quantifying the observed behaviors and theoretical claims are supported by numerical experiments. The analysis is then extended to a nonlinear model where the same two regimes are shown to exist and the resolution properties of the EMD are assessed.**

***Index Terms*—Empirical mode decomposition (EMD), resolution, spectral analysis, time frequency.**

I. Introduction

ONE standard issue in spectrum analysis is *resolution*, i.e., the capability of distinguishing between (more or less closely spaced) neighboring spectral components. At first sight, this question might appear as unambiguous, but a second thought suggests that it is the case only if some prior assumption on—or modeling of—the signal under consideration is given. Indeed, if it is known that the signal $x(t)$ to be analyzed actually consists of two tones of, say, equal amplitudes[1] with frequencies f_1 and f_2, one can write $x(t) = \cos 2\pi f_1 t + \cos 2\pi f_2 t$ and address the question of detecting and estimating f_1 and f_2. However, from a mathematical point of view, one can equally write $x(t) = 2\cos\pi(f_1 - f_2)t \cos\pi(f_1 + f_2)t$, with an underlying interpretation in terms of a single tone modulated in amplitude rather than of a superposition of two unimodular tones. As it is well known, such an interpretation is especially relevant when $f_1 \approx f_2$, a prominent example being given by the "beat effect" (see Fig. 1). In this respect, since, at some point, close tones are no longer perceived as such by the human ear but are rather considered as a whole, one can wonder whether a decomposition into tones is a good answer if the aim is to get a representation matched to physics (and/or perception) rather than to mathematics. More generally, if only $x(t)$ is given, there might be no *a priori* reason to prefer one of the two representations, the effective choice being in some sense driven by the way the signal is processed.

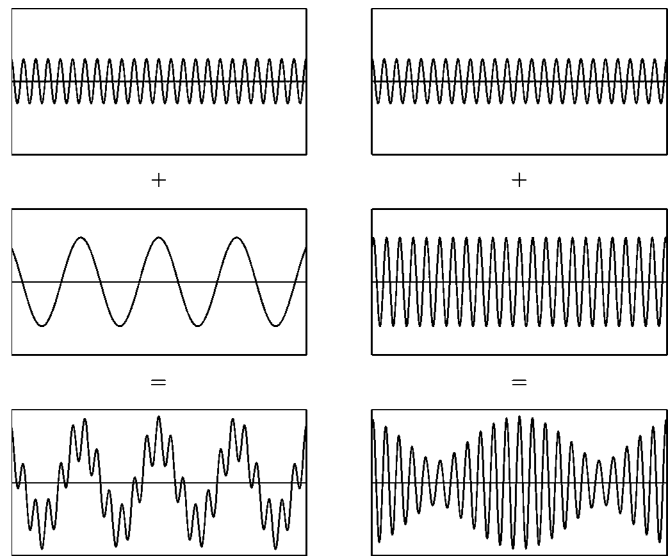

Fig. 1. *Beat effect*—In each column, signals in the bottom row are obtained as the superposition of the waveforms plotted in the top and middle rows. When the frequencies of the two superimposed tones are sufficiently far apart (left column), the two-tones interpretation is meaningful whereas, when they get closer (right column), an interpretation in terms of a single tone modulated in amplitude is clearly favored.

This question is addressed in this paper within the fresh perspective offered by the *empirical mode decomposition* (EMD) [1], [2], a relatively recent technique whose purpose is to adaptively decompose any signal into oscillatory contributions. Since the EMD is fully data driven, not model-based and only defined as the output of an iterative algorithm (see Section II), it is an open question to know what kind of separation can (or cannot) be achieved for two-tones composite signals when using the method. It is worth emphasizing that resolving closely spaced components is not the ultimate goal here and that poor resolution performance can indeed be accommodated provided that the decomposition is suitably matched to some physically meaningful interpretation. As for earlier publications [3], [4], the aim of the present study is primarily to contribute, within a well-controlled framework, to a better understanding of the possibilities and limitations offered by the EMD.

The paper is organized as follows. In Section II, the basics of the EMD are recalled. After having detailed the two-tones signal

Manuscript received November 13, 2006; revised June 13, 2007. The associate editor coordinating the review of this manuscript and approving it for publication was Dr. Peter Handel.

The authors are with the Physics Department (UMR 5672 CNRS), Ecole Normale Supérieure de Lyon, 69364 Lyon Cedex 07, France (e-mail: grilling@ens-lyon.fr; flandrin@ens-lyon.fr).

Color versions of one or more of the figures in this paper are available online at http://ieeexplore.ieee.org.

Digital Object Identifier 10.1109/TSP.2007.906771

[1]We restrict this Introduction to such an oversimplified case because situations with unequal amplitudes are computationally more complicated, while their interpretation remains essentially unchanged (see Fig. 1). For the same sake of simplicity in the discussion, phase differences are also ignored.

model and the performance measure used for quantifying the resolution capabilities of the EMD, Section III presents key features of results obtained by numerical simulations. Section IV then offers a theoretical analysis aimed at justifying the reported results, based on a careful study of extrema properties and interpolation schemes. Finally, an extension of the obtained results to simple nonlinear waveforms is proposed in Section V.

II. Empirical Mode Decomposition

In a nutshell, the EMD rationale can be summarized by the motto "signal = fast oscillations superimposed to slow oscillations," with iteration on the slow oscillations considered as a new signal. While this shares much with the wavelet philosophy, the important difference is that "fast" and "slow" components are not defined through some prescribed filtering operation but according to an algorithm that is overall rather close to an adaptive filtering operation. More precisely, the algorithm, referred to as the *sifting process* [1], iterates a nonlinear elementary operator $\mathcal{S}$ on the signal until some stopping criterion is met. Given a signal $x(t)$, the sifting operator $\mathcal{S}$ is defined by the following procedure.

1. Identify all extrema of $x(t)$.
2. Interpolate (using a cubic spline) between minima (respectively, maxima), ending up with some "envelope" $e_{\min}(t)$ (respectively, $e_{\max}(t)$).
3. Compute the mean $m(t) = (e_{\min}(t) + e_{\max}(t))/2$.
4. Subtract from the signal to obtain $\mathcal{S}[x](t) = x(t) - m(t)$.

If the stopping criterion is met after n iterations, the "fast" and "slow" components are defined, respectively, as $d_1[x](t) = \mathcal{S}^n[x](t)$ and $m_1[x](t) = x(t) - d_1[x](t)$. By construction, $d_1[x](t)$ is an oscillatory signal that in the EMD jargon is referred to as an "intrinsic mode function" (IMF) [1]. While an IMF is primarily defined as the output of EMD, a more usable definition is "a function whose local maxima are all positive, whose local minima are all negative, and whose envelopes (as defined in the sifting operator) are symmetrical with respect to the zero line." However, as argued in [5], only signals with constant envelopes fit the definition rigorously and consequently, the latter is generally considered in a loose sense. Concerning the "slow" component $m_1[x](t)$, on the other hand, all we know is that it locally oscillates more slowly than $d_1[x](t)$. We can then apply the same decomposition to it, leading to $m_1[x](t) = m_2[x](t) + d_2[x](t)$ and, recursively applying this on the $m_k[x](t)$, we get a representation of $x(t)$ of the form

$$x(t) = m_K[x](t) + \sum_{k=1}^{K} d_k[x](t) \tag{1}$$

with the decomposition ending when there are not enough extrema in $m_K[x](t)$ to define meaningful envelopes. The output of the EMD is thus *a priori* some sort of adaptive multiresolution decomposition [3]. In order to better assess the potential of the method (for which open source `Matlab/C` codes are available[2]), its behavior is illustrated in Fig. 2 on a synthetic signal. The results show that the EMD may be very efficient at naturally decomposing signals that are a burden to handle with usual methods based on Fourier or wavelet transform and often necessitate ad hoc solutions. The method proved useful in a variety of applications as diverse as climate variability [6], biomedical engineering [7], or blind-source separation [8].

[2][Online] Available: http://perso.ens-lyon.fr/patrick.flandrin/emd.html

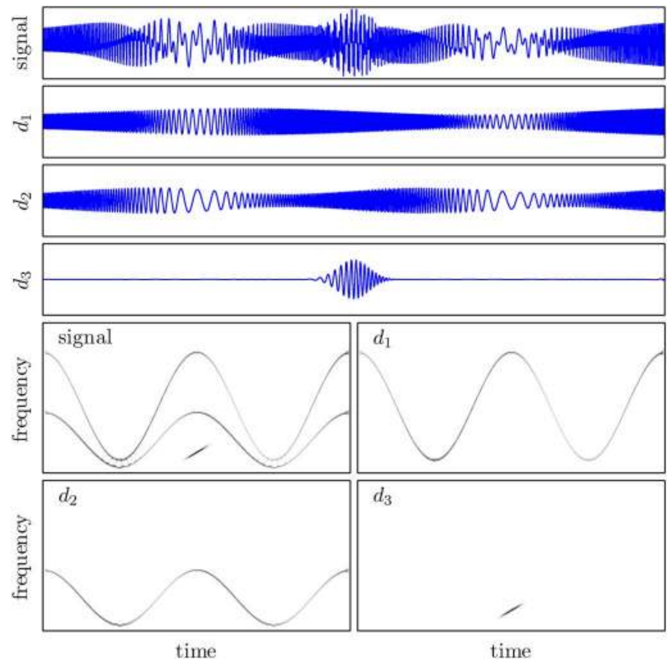

Fig. 2. *Synthetic three-component example*—The signal in the top row is decomposed by the EMD, resulting in the three IMFs listed below and six others that are not displayed since they are almost zero (they contain less than 0.3% of the total energy). The time-frequency analysis of the signal (top left of the four bottom diagrams) reveals three time-frequency signatures that overlap in both time and frequency, thus forbidding the components to be separated by any nonadaptive filtering technique. The time-frequency signatures of the first three IMFs extracted by EMD evidence that these modes efficiently capture the three-component structure of the analyzed signal. (All time-frequency representations are reassigned spectrograms.)

From a physical point of view, an IMF is a zero-mean oscillatory waveform, not necessarily made of sinusoidal functions and possibly modulated in both amplitude and frequency. Going back to the simple example sketched in Fig. 1, the zero-mean criterion makes of the composite signal in the right column a reasonable candidate for being already an admissible IMF, with no need for any further decomposition. This agrees with the beat effect interpretation and contrasts with the situation in the left column, where two zero-mean contributions are clearly visible, making of their identification a meaningful objective. It appears therefore that the EMD might be effective in the separation problem, as it has been formulated, and it is the purpose of this paper to switch from intuition and experimental facts to well-supported claims.

III. Experiments

In order to understand how the EMD decomposes a multicomponent signal into monocomponent ones, one can first remark that, because of the recursive nature of the algorithm, we only have to understand how the first IMF is extracted from the original signal. We will here adopt this perspective, with two-tones signals (in the spirit of Fig. 1) used for the tests. This will allow for analytically tractable analyses and offer an in-depth elaboration on the preliminary findings reported in [9].

A. Signal Model

As far as simulations are concerned, signals are discrete-time in nature and, in the situation we are interested in here, the most general form for a discrete-time two tones signal is

$$x[n] = a_1 \cos(2\pi f_1 n + \varphi_1) + a_2 \cos(2\pi f_2 n + \varphi_2), \quad n \in \mathbb{Z}.$$

We will, however, not use such a form with six parameters, since only three are needed without loss of generality. Concerning first the amplitudes a_1 and a_2, it is obvious that the behavior of the EMD only depends on their ratio $a \triangleq a_2/a_1$. A similar simplification applies as well to the two frequency and phase parameters $\{f_1, f_2\}$ and $\{\varphi_1, \varphi_2\}$ insofar as both frequencies are much smaller than the sampling frequency f_s. As reported in [9]–[11], sampling effects may turn the analysis much more complicated when the frequencies of the sinusoids get close to the Nyquist frequency $(f_1, f_2 \gtrsim 0.25 f_s)$. Therefore, we will only address the case where $f_1, f_2 \ll f_s$, allowing us to consider that we work with continuous-time signals. In that case, the covariance of the EMD with respect to time shifts and dilations makes its behavior only sensitive to the relative parameters $f \triangleq f_2/f_1$ and $\varphi \triangleq \varphi_2 - \varphi_1$, thus leading to the simpler continuous-time model:

$$x(t; a, f) = \cos 2\pi t + a \cos(2\pi f t + \varphi), \quad t \in \mathbb{R}. \tag{2}$$

As we can moreover restrain ourselves to the case $f \in]0, 1[$, the $\cos 2\pi t$ term will be referred to in the following as the higher frequency component (HF) and the $a\cos(2\pi f t + \varphi)$ term as the lower frequency component (LF).

B. Performance Measure

Given the above model, the questions of interest are 1) "When does the EMD retrieve the two individual tones?" 2) "When does it consider the signal as a single component?" and 3) "When does it do something else?"

In order to address the first question, we can consider the quantity

$$c_1^{(n)}(a, f, \varphi) \triangleq \frac{\left\| d_1^{(n)}(t; a, f) - \cos 2\pi t \right\|_{L^2(T)}}{\| a \cos(2\pi f t + \varphi) \|_{L^2(T)}} \tag{3}$$

where $d_1^{(n)}(t; a, f) \triangleq (\mathcal{S}^n x(\cdot; a, f))(t)$ stands for the first IMF extracted from $x(t; a, f)$ with exactly n sifting iterations and $\| \cdot \|_{L^2(T)}$ stands for the Euclidean norm on functions defined over $[0, T]$. When the two components are correctly separated, the fine to coarse nature of the decomposition ensures that the first IMF necessarily matches the HF component $\cos 2\pi t$. Provided this, the second IMF is bound to match the LF component because the first slow oscillations residual from which the second IMF is extracted already is the LF component. Therefore, a zero value of (3) indicates a perfect separation of the two components. Finally, the denominator is chosen so that the criterion has a value close to 1 when the two components are badly separated.

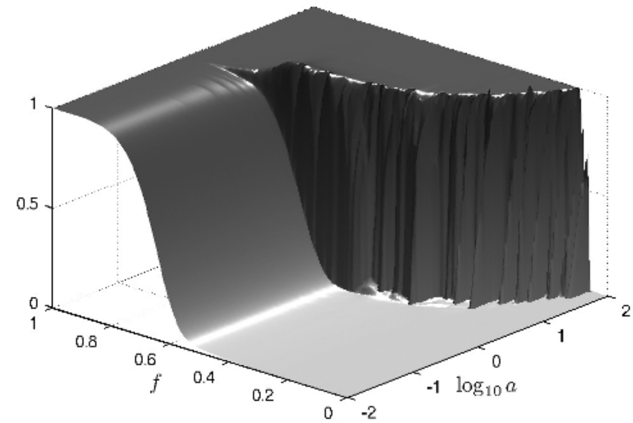

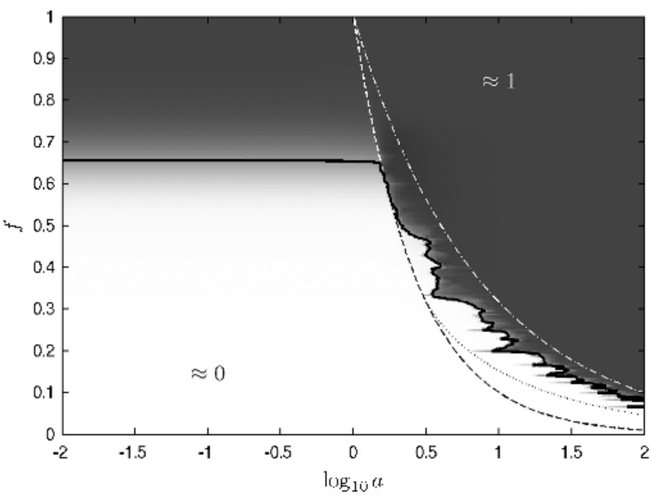

Fig. 3. *Performance measure of separation for two-tones signals*—A 3-D version of the averaged criterion (3) with $n = 10$ sifting iterations is plotted in the top diagram. Its 2-D projection onto the (a, f)-plane of amplitude and frequency ratios is plotted in the bottom diagram, with the critical curves predicted by theory superimposed as dashed $(af = 1)$, dashed–dotted $(af^2 = 1)$ and dotted $(af \sin(3\pi f/2) = 1)$ lines. The black thick line stands for the contour $\left\langle c_1^{(10)}(a, f, \varphi) \right\rangle_\varphi = 0.5$.

C. Results

Fig. 3 summarizes experimental results obtained for $\left\langle c_1^{(10)}(a, f, \varphi) \right\rangle_\varphi$, the averaged value over φ of $c_1^{(n)}(a, f, \varphi)$, with $n = 10$ sifting iterations.[3] Examining this figure evidences two rather well-separated domains with contrasting behaviors, depending on whether the amplitude ratio is greater or smaller than unity. While it seems rather natural that, for a given amplitude ratio, the EMD resolves the two frequencies only when the frequency ratio is below some cutoff, a less usual feature, coming from the highly nonlinear nature of the EMD, is that the cutoff frequency also depends on the amplitude ratio, in a nonsymmetrical way. What turns out is that this dependence essentially applies when the amplitude of the HF component gets smaller than that of the LF one, and vanishes in the opposite case. Moreover, there is a critical cutoff frequency ratio

[3]The corresponding standard deviation is not shown because it is generally very small, except in some very specific cases involving frequency synchronizations. The number of ten iterations is arbitrary, but its order of magnitude is guided by common practice [2].

($f_c \approx 0.67$ in the present case) above which it is impossible to separate the two components, whatever the amplitude ratio.

Those findings will be given a theoretical justification in Section IV. In particular, we will show in Section IV-B-1)-b) that the behavior of the EMD is very close to that of a linear filter when the amplitude ratio tends to zero and remains close as long as $a \leq 1$. The transfer function of this equivalent filter will be analytically characterized, and it will be shown that its cutoff frequency only depends on the number of sifting iterations.

IV. Theory

A. About Extrema

Extrema play a crucial role in the EMD algorithm, and it is important to discuss precisely what can be known about their locations and/or distributions. There are two asymptotic cases where we know exactly the locations of extrema: if the amplitude of one of the components is infinitely larger than that of the other one ($a \to 0$ or $a \to \infty$), then the locations of the extrema in the sum signal are exactly those of the extrema in the larger component. When the amplitude ratio is finite, locating precisely the extrema becomes tricky, but in almost all situations, we can still obtain the average number of extrema per unit length (or extrema rate) $r_e(a,f)$. This information will in fact serve as a basis for a theory that, while only asymptotically exact, adequately accounts for the behavior of the EMD for almost all frequency and amplitude ratios.

Proposition 1: If $af < 1$, $r_e(a,f) = 2$, i.e., the extrema rate is exactly the same as that of the HF component, whereas, if $af^2 > 1$, $r_e(a,f) = 2f$, i.e., it is exactly that of the LF one.

In order to prove those claims (illustrated in Fig. 4), the first step is to show that the sign of the second derivative of the two-tones signal at its extrema is actually the same as that of the second derivative of the HF component if $af < 1$ and that of the LF component if $af^2 > 1$. To this end, let us assume that $x(t;a,f)$ admits an extremum at $t = t_0$:

$$\partial_t x(t;a,f)|_{t=t_0} \propto \sin 2\pi t_0 + af \sin(2\pi f t_0 + \varphi) = 0. \quad (4)$$

The second derivative of $x(t;a,f)$ is

$$\partial_t^2 x(t;a,f) \propto \cos 2\pi t + af^2 \cos(2\pi f t + \varphi) \quad (5)$$

and what we want to justify is that

$$|af^2 \cos(2\pi f t_0 + \varphi)| < |\cos 2\pi t_0| \text{ if } af < 1,$$
$$|af^2 \cos(2\pi f t_0 + \varphi)| > |\cos 2\pi t_0| \text{ if } af^2 > 1.$$

Squaring the above equations and replacing $\cos^2 2\pi t_0$ in both of them by its value from (4), we obtain

$$a^2 f^4 \cos^2(2\pi f t_0+\varphi) + a^2 f^2 \sin^2(2\pi f t_0+\varphi) < 1 \text{ if } af < 1,$$
$$a^2 f^4 \cos^2(2\pi f t_0+\varphi) + a^2 f^2 \sin^2(2\pi f t_0+\varphi) > 1 \text{ if } af^2 > 1$$

which hold true since $a^2 f^4 < a^2 f^2 < 1$ if $af < 1$ and $1 < a^2 f^4 < a^2 f^2$ if $af^2 > 1$. Given this result, there can only be one extremum between two successive zero-crossings of the second derivative of the HF (respectively, LF) component if $af < 1$ (respectively, $af^2 > 1$) because its type (maximum or minimum) is determined by the sign of the second derivative of the HF (respectively, LF) component. Thus, there can only be one extremum per half-period of the HF (respectively, LF) component, hence the extrema rates and the conclusion of the proof.

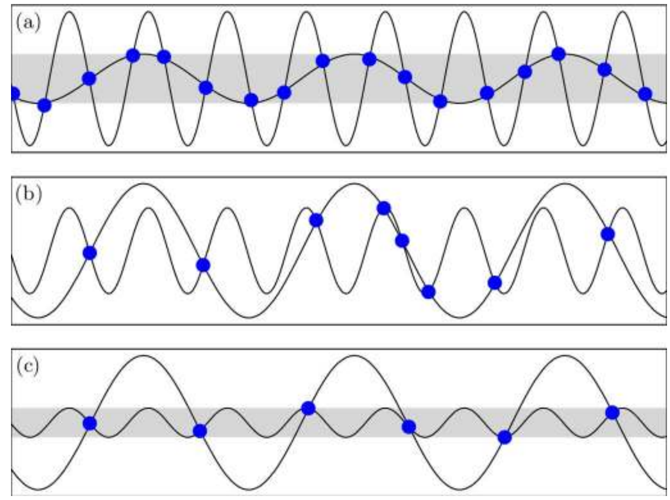

Fig. 4. *Locations of the extrema in the two-tones signal*—In each graph are plotted the derivative of the HF component and the *opposite* of the derivative of the LF component so that each crossing corresponds to an extremum in the composite signal. (a) $af < 1$: as the amplitude of the derivative of the HF component is greater than that of the LF component, there is exactly one crossing between two successive extrema of the HF component; (b) $af > 1$ and $af^2 < 1$: no regular distribution of the crossings can be guaranteed; and (c) $af^2 > 1$: as the maximum slope of the derivative of the LF component is greater than that of the HF component, there is exactly one crossing between two successive extrema of the LF component.

Indeed, it seems rather natural that the EMD can only extract a component if it "sees" extrema that are related to it. Therefore, it seems unlikely to recover the HF component in the $af^2 > 1$ area as the signals extrema are more related to the LF component. On the other hand, recovering the HF component in the $af < 1$ area seems feasible *a priori*. As extracting the highest frequency component into the first IMF is what we intuitively expect the EMD will do, we can think of the $af < 1$ area as a "normal" case while the $af^2 > 1$ area can be viewed as "abnormal." We will see in the following that quite strange behaviors can indeed be observed in that area. However, the existence of such an "abnormal" domain is far from a complete drawback as it allows in particular to preserve nonlinear periodic waveforms as single IMFs instead of scattering their harmonics over several ones.

The two curves, $af = 1$ and $af^2 = 1$, have been superimposed to the diagram Fig. 3 in order to visualize the link between them and the behavior of the EMD. It appears indeed that the $af^2 = 1$ curve tightly delimits the upper side of the transition area in the right side of the figure. On the other hand, the $af = 1$ curve delimiting the lower side is not as tight as soon as $f < 1/3$. A refinement resulting in a closer theoretical boundary when $f < 1/3$ will be proposed in Section IV-C.

Finally, in order to better support the theory exposed in Section IV-B, some control can be added to the extrema locations. Indeed, if we take into account that the crossings in

Fig. 4(a) can only occur in the shaded band, then it results that each crossing is distant from a zero-crossing of the HF component by at most $1/(2\pi)\sin^{-1}(af)$. In terms of extrema, this exactly means that, when $af < 1$, each extremum is distant from an extremum of the HF component by at most $1/(2\pi)\sin^{-1}(af)$. Likewise, when $af^2 > 1$, each extremum can be shown to be distant from an extremum of the LF component by at most $1/(2\pi f)\sin^{-1}(1/af)$. In both cases, these statements give some quantitative control on the extrema locations supporting the idea that these are close to those of one of the two components as soon as af gets sufficiently smaller than 1 or alternatively af^2 sufficiently larger than 1.

B. *Model for the EMD When the Extrema Are Equally Spaced*

Based on the above statements regarding extrema, the model proposed here relies on the only assumption that extrema are located at the exact same places as those of one of the two components (the HF one when $af < 1$ or the LF one when $af^2 > 1$).

1) Case $af < 1$:

a) Derivation of the Model: The model assumes that maxima are located at integer time instants $k, k \in \mathbb{Z}$ while minima are located at half-integer ones $k + 1/2, k \in \mathbb{Z}$. The extrema being equally spaced, the set of maxima (or minima) can be seen as a specific sampling of the initial signal at the frequency of the HF component, which is 1 in our simplified model. In the Fourier domain, the Dirac combs associated with the maxima and minima samplings are

$$\begin{aligned}\mathrm{III}_{\max}(\nu) &= \sum_{k\in\mathbb{Z}} \delta(\nu - k)\\ \mathrm{III}_{\min}(\nu) &= \sum_{k\in\mathbb{Z}} (-1)^k \delta(\nu - k). \end{aligned} \tag{6}$$

where the $(-1)^k$ term comes from the time shift between the two samplings. Convolving these with the signal in the Fourier domain, we obtain the Fourier representations of the maxima/minima sets (respectively, $S_{\max}$ and $S_{\min}$):

$$S_{\max/\min}(\nu) = \left(\mathrm{III}_{\max/\min} * \hat{x}\right)(\nu).$$

If we then use an interpolation scheme that, when the interpolation points (usually referred to as "knots") are equally spaced can be expressed in terms of digital filtering (e.g., Shannon, splines, etc.) with frequency response $I(\nu)$ for unit spaced knots, the envelopes ($e_{\max}(t)$ and $e_{\min}(t)$) have the Fourier representations

$$\hat{e}_{\max/\min}(\nu) = I(\nu)\left(\mathrm{III}_{\max/\min} * \hat{x}\right)(\nu).$$

This implies that

$$\frac{\hat{e}_{\min}(\nu) + \hat{e}_{\max}(\nu)}{2} = I(\nu)\left(\mathrm{III}_{\mathrm{mean}} * \hat{x}\right)(\nu)$$

where $\mathrm{III}_{\mathrm{mean}}(\nu) = \sum_{k\in\mathbb{Z}} \delta(\nu - 2k)$, the two interleaved samplings being replaced by another one with double frequency. It is worth noticing that the samplings (6) introduce aliasing as soon as the signal contains frequencies above the corresponding Nyquist frequency 0.5 (such effects have been first reported in [12]) but, in the present case, the cancellation of the odd indexes in the Dirac combs cancels the aliasing effects provided the spectrum of the signal is zero outside of $[-1, 1]$. While this last condition is obviously met in the case of the two-tones signal when $af < 1$, it will not be the case in the following when $af^2 > 1$, and furthermore when we will consider nonlinear waveforms.

Finally, we end up with a Fourier representation of the first iteration of the sifting operator given by

$$(\widehat{\mathcal{S}x})(\nu) = \hat{x}(\nu) - I(\nu)\left(\mathrm{III}_{\mathrm{mean}} * \hat{x}\right)(\nu). \tag{7}$$

As our only assumption was about the locations of extrema, this representation (or a properly dilated one) holds as soon as the extrema locations are nearly equally spaced.

b) Expressions of the IMFs: The signal (2) initially contains four Fourier components at 1, -1, f, $-f$ with coefficients $c_{\pm 1} = 1/2$, and $c_{\pm f} = ae^{\pm i\varphi}/2$. After one iteration of the sifting operator, the latter ones become $c_{\pm 1}^{(1)} = 1/2$ and $c_{\pm f}^{(1)} = (1 - I(f))ae^{\pm i\varphi}/2$, while some new Fourier components appear at $2k \pm f, k \in \mathbb{Z}^*$, because of the extrema sampling. Fortunately, the associated coefficients $c_{2k\pm f} = -I(2k \pm f)ae^{\pm i\varphi}$ are generally very small as $I(\nu)$ is typically close to zero when $|\nu| > 1$. Therefore, those aliased components can generally be neglected, thus implying that the model (7) can be well approximated by a simple *linear filter* with frequency response $1 - I(\nu)$. As $I(\nu)$ typically stays in the range $[0, 1]$ for usual interpolation schemes, the signal after one iteration is then close to a two-tones signal (2), with the same frequency ratio f, a smaller amplitude ratio $a^{(1)} < a$ and the same phase. Thus, the condition $af < 1$ is even better satisfied after one iteration, and so the model (7) still holds for all the possible following sifting iterations. This allows us to finally express the first IMF obtained after n iterations in the linear approximation as

$$\begin{aligned} d_1^{(n)}(t; a, f) &= (\mathcal{S}^n x(.; a, f))(t)\\ &= \cos 2\pi t + (1 - I(f))^n a \cos(2\pi f t + \varphi) \end{aligned} \tag{8}$$

and, consequently, the second (and last) IMF as

$$\begin{aligned} d_2^{(n)}(t; a, f) &= x(t; a, f) - d_1^{(n)}(t; a, f)\\ &= (1 - (1 - I(f))^n)\, a \cos(2\pi f t + \varphi). \end{aligned}$$

In the case of cubic spline interpolation, which is by far the most commonly used for the EMD, it follows from [13] that the frequency response for unit spaced knots $I(\nu)$ is given by

$$I^{c.s.}(\nu) = \left(\frac{\sin \pi\nu}{\pi\nu}\right)^4 \frac{3}{2 + \cos 2\pi\nu}.$$

Combining this with (8) finally yields a theoretical model for the left side ($af < 1$) of Fig. 3, which is compared to simulations for different numbers of iterations and amplitude ratios in Fig. 5. According to these results, both the model and the simulations point out that the EMD performs as a linear filter (high-pass for the first IMF, low-pass for the second one) whose

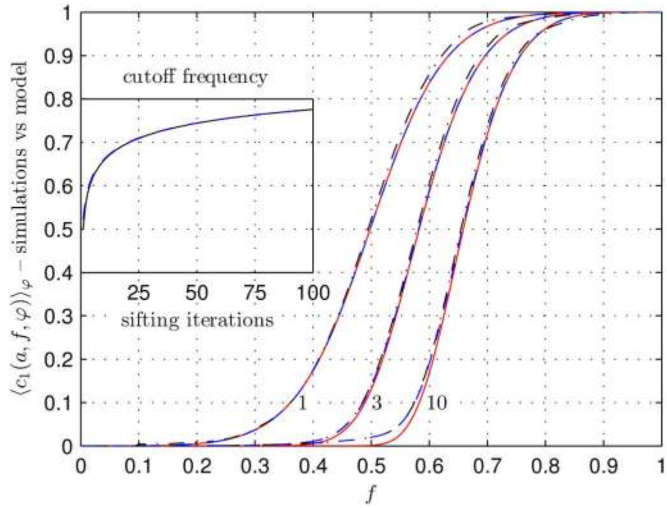

Fig. 5. *Equivalent filter model for the EMD*—Experimental results for $\left\langle c_1^{(n)}(a,f,\varphi)\right\rangle_\varphi$ (solid line curves) are compared to theoretical predictions when $a = 10^{-2}$ (dashed curve) and $a = 1$ (dashed–dotted curve), for $n = 1$, 3, and 10 sifting iterations. In the small box are plotted the exact value of the cutoff frequency (solid line curve) and its approximation (9) (dashed curve), as a function of the number of sifting iterations.

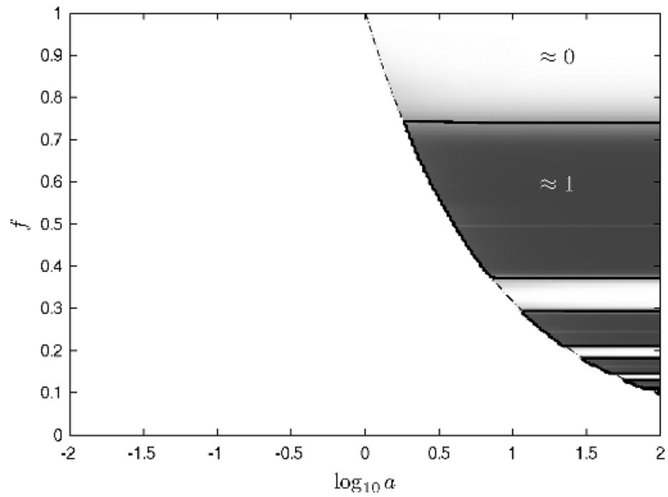

Fig. 6. *Performance measure of separation for two-tones signals*—The averaged value of the criterion (10) is plotted for $n = 10$ sifting iterations. Only the $af^2 > 1$ area is displayed because the criterion is meaningless otherwise. As in Fig. 3, the black thick line stands for the contour $\left\langle c_2^{(10)}(a,f,\varphi)\right\rangle_\varphi = 0.5$.

cutoff frequency only depends on the frequency of the HF component and on the number of sifting iterations. It appears moreover that the model remains very close to the simulation results even when af gets close to 1 (i.e., when the model assumption of equally spaced extrema clearly becomes questionable), thus supporting the claim that the EMD acts almost as a linear filter over the whole range $af < 1$.

c) Approximation of the Cutoff Frequency: A natural definition for the cutoff frequency $f_c^{(n)}$ (where n stands for the number of iterations) is the value for which the response of the EMD equivalent filter is half its maximum, as follows:

$$\left(1 - I\left(f_c^{(n)}\right)\right)^n = \frac{1}{2}.$$

There is unfortunately no analytical solution to this equation in the case of cubic spline interpolation, but a good approximation is given by the following asymptotic formula:

$$f_c^{(n)} = \left(1 + \left(\frac{\ln 2}{n}\right)^{(1/4)}\right)^{-1} + O\left(n^{-(5/4)}\right). \tag{9}$$

As pointed out by this expression, the cutoff frequency is a nondecreasing function of the number of iterations that furthermore tends to 1 when n tends to infinity. The increase is, however, very slow, and therefore the cutoff frequency remains significantly lower than 1 for reasonable numbers of iterations: typically $f_c^{(n)} \lesssim 0.75$ when $n \lesssim 100$ (see Fig. 5). Since this cutoff frequency is related to a notion of *relative frequency resolution*, our results agree with the practical observations that suggest a rather poor value for the latter, typically about 0.5. Moreover, the enhancement of that resolution when n is increased, though rather weak, is consistent with empirical observations stating that increasing n increases the number of IMFs and smoothes the envelopes variations. Indeed, both features are consistent with a decrease of each IMF bandwidth, at least locally.[4]

2) Case $af^2 > 1$:

a) Simulations: In the area $af^2 > 1$, we know from the simulation results (Fig. 3) that the EMD can never retrieve the two tone components. Thus, the next question of interest here is the second one: Does the EMD consider the signal as a single modulated component or not? If the answer is "yes," the first IMF should be the original signal, so that we can address the question by examining the following distance measure (the choice for normalization will become clear later):

$$c_2^{(n)}(a,f,\varphi) \triangleq \frac{\left\| d_1^{(n)}(t;a,f) - x(t;a,f)\right\|_{L^2(T)}}{\|\cos 2\pi t\|_{L^2(T)}}. \tag{10}$$

As can be observed in Fig. 6, the behavior of the EMD when $af^2 > 1$ seems to depend mostly on the frequency ratio. More precisely, it appears that the value of $\left\langle c_2^{(10)}(a,f,\varphi)\right\rangle_\varphi$ is either close to one or close to zero depending on whether f is close to $(2k)^{-1}$ or $(2k+1)^{-1}$, $k \in \mathbb{N}^*$. This means that the EMD effectively considers the signal as a single component when f is close to $(2k+1)^{-1}$ but does something else when f is close to $(2k)^{-1}$. We will show in Section IV-B-2)-b) that in the latter case, the aliasing effects resulting from the extrema sampling actually give birth to a new lower frequency component.

b) The Model: As before, the model assumes that the extrema are equally spaced and therefore the former reasoning applies. We then end up with a formulation which is basically the same as in (7), with a few adjustments, as follows:

$$(\widehat{\mathcal{S}x})(\nu) = \hat{x}(\nu) - I\left(\frac{\nu}{f}\right)\left(\text{III}_{\text{mean}} * \hat{x}\right)(\nu) \tag{11}$$

with $\text{III}_{\text{mean}}(\nu) = \sum_{k\in\mathbb{Z}} \delta(\nu - 2kf)e^{i2k\varphi}$.

[4]However, it has to be noted that, as argued in [5], increasing with no limit the number of sifting iterations would result in IMFs with no amplitude modulation.

c) Expressions of the IMFs: If we now apply this model to the two-tones signal, the four Fourier coefficients $c_{\pm 1} = 1/2$ and $c_{\pm f} = ae^{\pm i\varphi}/2$ become after one sifting iteration $c_{\pm 1} = (1 - I(1/f))/2$ and $c_{\pm f} = ae^{\pm i\varphi}/2$. As in the former case, the component that has its extrema close to those of the multicomponent signal is left unchanged by the sifting operator while the other one has its amplitude decreased. However, the decrease is almost nonexistent here because $1/f > 1$ and therefore $I(1/f) \approx 0$. Thus, the four initial Fourier components are nearly left unchanged after the first iteration. This would be fine if there were no aliased components as in the first case but, unfortunately, there are. Indeed, if $k_f \in \mathbb{N}$ is such that $2k_f - 1 < 1/f < 2k_f + 1$, there are two aliased frequencies $f_a = 2k_f f - 1$ and its negative that both lie in $[-f, f]$ and might therefore not be removed by the interpolation filter $I(\nu/f)$. According to our model, the first IMF is then

$$d_1^{(1)}(t; a, f) = x(t; a, f) - I\left(\frac{f_a}{f}\right) \cos\left(2\pi f_a t + 2k_f \varphi\right).$$

As this new component has smaller frequency and amplitude than the HF component, we can expect the extrema in the IMF after one iteration to still be near those of the LF component. The aliased component has therefore little impact and can be neglected too. According to this model, the IMF obtained after n iterations is then

$$d_1^{(n)}(t; a, f) = x(t; a, f) - \lambda_n \cos\left(2\pi f_a t + 2k_f \varphi\right) \quad (12)$$

with $\lambda_n = 1 - (1 - I(f_a/f))^n$ and, consequently

$$d_2^{(n)}(t; a, f) = \lambda_n \cos\left(2\pi f_a t + 2k_f \varphi\right).$$

Unlike the case $af < 1$, these expressions show that there is no possible linear filtering equivalent for the EMD when $af^2 > 1$.

As a matter of fact, the behavior of the EMD is rather odd as it just creates a new lower frequency component which is added to the signal to obtain the first IMF, and then compensated in the second one. Moreover, that new frequency is even more annoying when it comes to interpretation as it might be mistaken for an intrinsic time scale of the signal while its relevance is rather questionable. Indeed, if the EMD is followed by instantaneous frequency/amplitude estimation, as in the Hilbert–Huang Transform framework [1], [2], this results in a first IMF with an instantaneous frequency that oscillates around f while that of the second IMF is exactly f_a. Ultimately, the unfortunate EMD user might uncover a component at f_a, while the frequency of the corresponding intrinsic oscillation is in fact 1!

Quantitatively, the amplitude λ_n of the new frequency component depends on the ratio f_a/f. In a first approximation, $f_a/f \lesssim f_c^{(n)} \Rightarrow \lambda_n \approx 1$ while, on the other hand, $f_a/f \gtrsim f_c^{(n)} \Rightarrow \lambda_n \approx 0$. This means that the new component has either an amplitude close to that of the original at frequency 1 when f is close to $(2k)^{-1}, k \in \mathbb{N}^*$ or an almost zero amplitude when f is close to $(2k+1)^{-1}$. Moreover, as the cutoff frequency $f_c^{(n)}$ increases with n, the width of the bands where $\lambda_n \approx 1$ also increases with n.

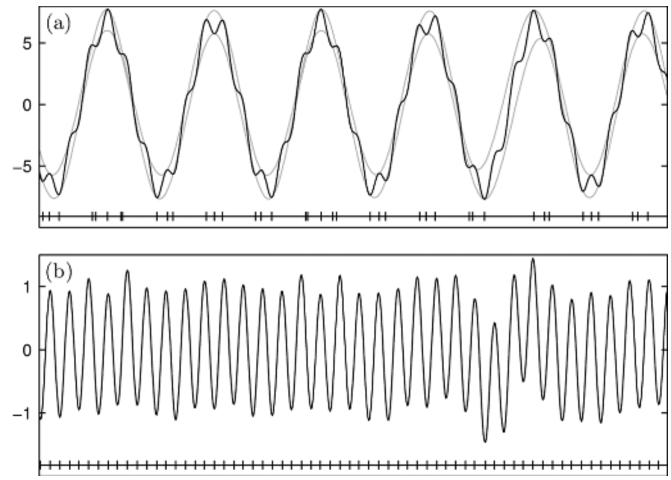

Fig. 7. *Example of a two-tones signal with $af \gtrsim 1$ and $f < 1/3$*—As it can be seen in (a), some extrema of the HF component do not give birth to extrema in the composite signal (identified as marks on the horizontal line at the bottom of the diagram) but only to inflexions surrounded by humps. However, since the lower and upper envelopes (light gray lines) roughly follow the LF trend, their mean is close to the latter and subtracting it from the composite signal uncovers the hidden extrema: this is evidenced in (b), which plots the first IMF after one sifting iteration and the associated distribution of its extrema.

C. Refinements When $f < 1/3$

1) Extrema May Appear During the Sifting Process: In Section IV-A, we showed that the two curves $af = 1$ and $af^2 = 1$ are the boundaries of a transition area for the extrema density. Among these curves, we also noticed that $af = 1$ delimits the lower side of the transition area but rather loosely when $f < 1/3$. In that area, it appears that even if the extrema rate is slightly below 2 ($af \gtrsim 1$), the EMD acts as if the extrema were close to those of the HF component. *The explanation for this behavior is in fact that some extrema may appear when iterating the sifting process*. As a matter of fact, a close look at the two-tones signal when $af > 1$ and $af^2 < 1$ (see Fig. 7) shows that its extrema rate, which is between those of the two tones, is not uniform: the extrema are mostly located around the extrema of the LF component. Besides, the signal also exhibits strong inflections related to extrema pairs of the HF component that clearly would yield extrema pairs in the sum signal if the amplitude ratio was smaller. As the signal exhibits local minima (respectively, maxima) around what appears to be the maxima (respectively, minima) of the LF component, its lower (respectively, upper) envelope and, therefore, their mean roughly follow the shape of the LF component. Subtracting this mean from the signal then naturally reveals the extrema that were hidden as inflections, and it follows that the extrema rate may increase after one sifting iteration to match the rate of the HF component, thus allowing us to use the model (7) for the remaining iterations.

2) Tighter Boundary for the Transition Area: It follows from Proposition 1 that, for a given f, the number of extrema in the two-tones signal that lie in between two successive zero-crossings of the LF component is close to $1/f$ if $a < 1/f$ and exactly 1 if $a > 1/f^2$. However, the threshold value of a below which this number is at least 2 is in fact lower than $1/f^2$ and higher than $1/f$ if $f < 1/3$. It is graphically clear that this threshold

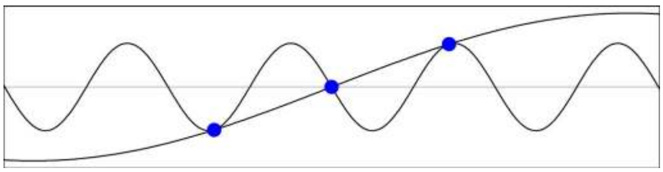

Fig. 8. *Limit case situation* $a = \tilde{a}(f)$—Like in Fig. 4, the derivative of the HF component is plotted together with the opposite of the derivative of the LF component. If $a < \tilde{a}(f)$, it is graphically clear that whatever the value of φ, there can not be less than three extrema in $x(t; a, f)$ (big dots) between two zero-crossings of the LF component (extrema of the derivative in the figure). Conversely, if $a > \tilde{a}(f)$, it is clearly possible to see only one extremum in the same range.

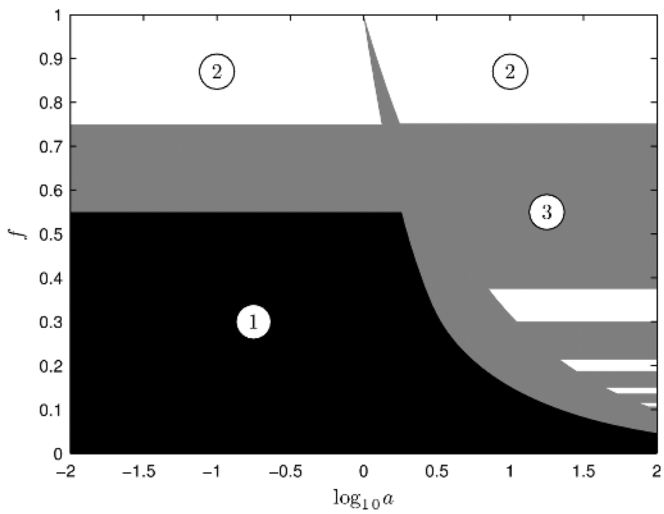

Fig. 9. *Summary of the EMD answers to the two-tones separation problem*—Depending on the frequency ratio f and the amplitude ratio a, three domains with different behaviors can be distinguished: 1) the two components are separated and correctly identified, 2) they are considered as a single waveform, and 3) the EMD does something else.

$\tilde{a}(f)$ follows from a tangency condition in the worst case situation (see Fig. 8). Although this condition admits no analytical solution, assuming that the tangency points coincide with the extrema of the HF components derivative leads to the approximation

$$\tilde{a}(f) \approx \left(f \sin\left(\frac{3\pi f}{2}\right)\right)^{-1}$$

and, hence, to the improved boundary reported on Fig. 3.

D. Summary

Thanks to the previous analysis, we are finally able to answer the three initial questions of interest. A schematic view of the EMD answers to the two-tones separation problem is proposed in Fig. 9, where each area is labelled according to one of the three following possibilities: 1) the two components are well separated and correctly identified, 2) their sum is left unchanged and considered as a single waveform, and 3) the EMD does something else, either halfway between 1) and 2), or with the possibility of a decomposition in fake oscillations different from the effective tones.

V. Some Generalizations Beyond Tones

The previous analysis showed that it was possible to describe the behavior of the EMD with a simple analytical model provided that the extrema were nearly equally spaced. As the model only requires that last condition to hold, it should also hold if the waveforms of the two components slightly deviate from a sinusoid. As a generalization, we will now consider simple nonlinear waveforms with two symmetrically interleaved extrema per period. Thus, the new signal model in the following is

$$x(t; a, f) = x_1(t) + a x_2(ft + \varphi)$$

where $x_1(t)$ and $x_2(t)$ are two unit-period functions with two symmetrically interleaved extrema per period, also defined by their Fourier expansions

$$x_j(t) = \sum_p c_{j,p} e^{2p\pi i t}.$$

Since our goal is to study the possible separation of the two components by the EMD, we will also require that both $x_j(t)$ already are IMFs so that a perfect separation can *a priori* be achieved. Therefore, we will assume that the value of a component at its maxima is the opposite of its value at its minima.

A. Theory

In this section, we provide two results: we prove in a general setting the existence of the two asymptotic domains, where extrema are close to those of one of the two components, and we also derive the first IMF in the case where the extrema of the HF component are equally spaced. However, we only provide a model for the "normal" case where the extrema are close to those of the HF component because it is the only case in which the EMD may accurately retrieve the two components. On the other hand, we could show that the behavior of the EMD in the "abnormal" area is similar to the sinusoidal case as it still adds new aliased components to the signal to build the first IMF and then subtracts them in the second one. The difference is just that there may be more aliased frequencies, one for each harmonic of the HF component.

Proposition 2: Let $x_1(t)$ and $x_2(t)$ be two periodic and at least two-times continuously differentiable functions. If each function $x_i(t)$ has the property that for some positive (η, ϵ), $|\partial_t x_i(t)| < \eta \implies |\partial_t^2 x_i(t)| > \epsilon$,[5] then the locations of the extrema of $x(t; a, f) = x_1(t) + a x_2(ft + \varphi)$ are those of $x_1(t)$ when $|a| \to 0$ and those of $x_2(ft + \varphi)$ when $|a| \to \infty$. Moreover, there are two positive numbers A and B such that for all $(f, \varphi) \in [0, 1] \times \mathbb{R}$, the extrema rate of $x(t; a, f)$ is the same as that of $x_1(t)$ when $|af| < A$ and the same as that of $x_2(ft + \varphi)$ when $|af^2| > B$

The proof is given in the Appendix. Assuming that the proposition holds, the model (7) should be valid when $a \to 0$ and hopefully remain acceptable over the "normal" domain, if the HF component $x_1(t)$ has equally spaced extrema. The derivation of the IMFs is then very similar to the sinusoidal case,

[5]For nonpathological functions, this only means that the derivative and second-derivative cannot be zero at the same time.

with additional aliasing effects. First we can show that the first IMF always contains the HF component. If we assume $x_1(t)$ has maxima at integer time instants and minima at half-integer ones, the Dirac combs associated to samplings are exactly the same as in Section IV-B-1) and thus[6]

$$
\begin{aligned}
(\widehat{\mathcal{S}x_1})(\nu) =& \widehat{x_1}(\nu) - I(\nu) \\
& \times \left(\left(\sum_p c_{1,2p} \right) \sum_{n\in\mathbb{Z}} \delta(\nu - 2n) \right. \\
& \left. + \left(\sum_p c_{1,2p+1} \right) \sum_{n\in\mathbb{Z}} \delta(\nu - 2n + 1) \right), \\
=& \widehat{x_1}(\nu) - \delta(\nu) \sum_p c_{1,2p} = \widehat{x_1}(\nu)
\end{aligned}
$$

since $x_1(t)$ is an IMF with maximum value $x_1(0) = \sum_p c_{1,p}$ and minimum value $x_1(0.5) = \sum_p (-1)^p c_{1,p}$. Hence, the HF component is left unchanged by the sifting operator.

If we now focus on the LF component, each Fourier coefficient at frequency pf can give birth to a set of aliased frequencies at $2k + pf$, among which only one is in the range $[-1, 1]$ where the interpolation filter is non-negligible. If $k_{p,f}$ is the integer such that $2k_{p,f} + pf \in [-1, 1]$, then

$$
\begin{aligned}
(\widehat{\mathcal{S}x_2})(\nu) =& \hat{x}(\nu) - I(\nu) \left(\sum_p c_{2,p} \delta(\nu - pf - 2k_{p,f}) \right), \\
=& \hat{x}(\nu) - \sum_p c_{2,p} I(pf + 2k_{p,f}) \delta(\nu - pf - 2k_{p,f}).
\end{aligned}
$$

Thus, after one sifting iteration, the signal contains the HF component, some harmonics of the LF component and possibly aliased frequencies. Since the possible aliased components have smaller amplitudes than the original harmonics, we can expect that the extrema in the signal after one sifting iteration are still close to those of the HF component. Given this, the model (7) should still be valid for the following sifting iterations thus allowing to finally express the first IMF after n iterations:

$$
d_1^{(n)}(t) = x(t) - \sum_p \lambda_p^{(n)} c_{2,p} e^{2i\pi(pf + 2k_{p,f})t}
$$

where $\lambda_p^{(n)} = 1 - (1 - I(pf + 2k_{p,f}))^n$. We do not express the second IMF here since $x(t) - d_1^{(n)}(t)$ is not necessarily an IMF like it was in the sinusoidal case. In the following, the two components will be considered correctly separated iff $d_1(t) = x_1(t)$.

From the expression of the first IMF, we can already predict when the EMD will be able to accurately separate the two components: *all the harmonics of the LF component must have a frequency lower than* $f_c^{(n)}$. Indeed, this implies that all $k_{p,f}$ are zero and $\lambda_p^{(n)} \approx 1$ which means that the first IMF is $x(t)$ minus the LF component, and is therefore the HF component. On the other hand, there is often no domain where the composite signal is considered a single IMF because of the possible aliased components.

[6]We write here that $\mathcal{S}x(t) = \mathcal{S}x_1(t) + a\mathcal{S}x_2(ft + \varphi)$ which, in theory, would truly hold if the extrema sampling was the same for both components.

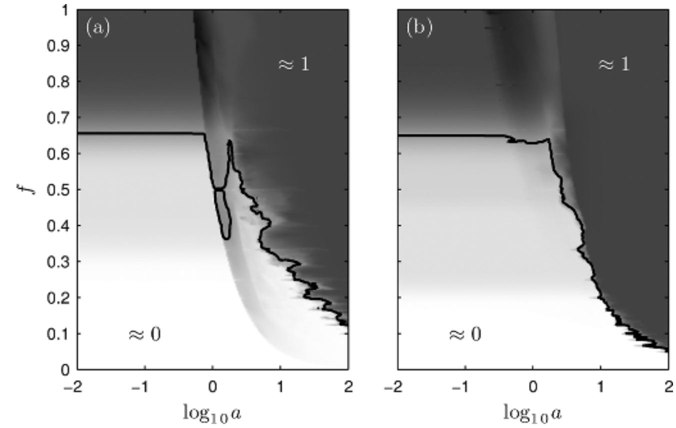

Fig. 10. *Performance measure of separation for nonlinear signals with two equally spaced extrema per period*—Averaged value of the criterion (13) as a function of the amplitude and frequency ratios for ten sifting iterations: (a) $x_1(t) = s_1(t)$, $x_2(t) = s_2(t)$; (b) $x_1(t) = s_2(t)$, $x_2(t) = s_1(t)$. The black thick lines stand for the contour lines $\left\langle c_1^{(10)}(a, f, \varphi) \right\rangle_\varphi = 0.5$.

B. Examples

For the sake of simplicity, the example signals used in this paper only have two Fourier components, fundamental and second or third harmonic, but the proposed model remains valid for more complicated signals. The two nonlinear waveforms that will be used in the following are

$$
\begin{aligned}
s_1(t) &= \cos(2\pi t) + 0.15\cos(6\pi t) \\
s_2(t) &= \cos(2\pi t) - 0.15\cos(4\pi t) + 0.15
\end{aligned}
$$

where the last constant ensures that $s_2(t)$ is already an IMF. The criterion

$$
c_1^{(n)}(a, f, \varphi) \triangleq \frac{\left\| d_1^{(n)}(t; a, f) - x_1(t) \right\|_{L^2(T)}}{\| a x_2(ft + \varphi) \|_{L^2(T)}} \tag{13}
$$

is plotted in Fig. 10 as a function of the amplitude and frequency ratios with $x_1(t) = s_1(t)$ and $x_2(t) = s_2(t)$ in Fig. 10(a) and conversely in Fig. 10(b).

As can be seen in both figures, as soon as the amplitude ratio is small or large enough, the behavior of (13) depends almost only on the frequency ratio. A more thorough study would show that this in fact coincides with areas where the extrema rate is the same as one of the two components. Compared to the sinusoidal case, we also notice that the transition area between these two domains is much wider. The reason for this is in fact that the width of the transition area in the sinusoidal case is a minimum width.

If we now focus on the behavior of the decomposition in the "normal" area, we can observe the same global behavior as in the sinusoidal case, but it also appears that the value of the criterion significantly departs from zero for much smaller frequency ratios. This is, in fact, caused by the harmonics in the LF component that are incorrectly assigned to the first IMF as soon as their frequency is higher than the cutoff frequency. Thus, the smooth step around $f \approx 0.32$ in Fig. 10(a) corresponds to the second harmonic of LF that is assigned to the first IMF as soon as $2f \geq f_c^{(10)} \approx 0.65$. Similarly the smooth step around $f \approx 0.22$ in Fig. 10(b) corresponds to the third harmonic of LF crossing the cutoff frequency. Aliased frequencies may also be present in that figure as soon as $3f > 1$. In fact these correspond to the barely visible smooth step around $f \approx 0.45$ in Fig. 10(b) because this also means that $2 - 3f \approx f_c^{(10)}$. A similar smooth step should be observable too in Fig. 10(a) around $f \approx 0.65$ $\left(2 - 2f \approx f_c^{(10)}\right)$ but it is hidden by the big step corresponding to the fundamental.

VI. Conclusion

This study has first considered in detail the way the EMD behaves in the simple case of a two-tones signal and then extended the results to a simple nonlinear model. A number of experimental findings, well supported by a theoretical analysis, have been reported. This allows for a better understanding of the method and of its relevance in terms of adequation between the mathematical decomposition it provides and its physical interpretation. More precisely, one prominent outcome of the study in the two-tones case is that the EMD allows one to address in a fully data-driven way the question whether a given signal is better represented as a sum of two separate, unmodulated tones, or rather as a single, modulated waveform, with an answer that turns out to be in good agreement with intuition (and/or perception).

A limitation of the present study is of course the model on which it is based, which can be thought of as oversimplified and unrealistic. However, following from the very local nature of the EMD we expect that conclusions drawn from the study of unmodulated tones still apply to slowly-varying AM–FM situations (see, e.g., Fig. 2).

Another possible extension is related to the model (7), which is close to a linear filter: a popular situation where such a model has been proposed is broadband noise, where it has appeared that the EMD acts as a quasi-dyadic filter bank [4], [14]. Unlike the two-tones case, however, the equivalent filters for broadband noise have only been characterized by numerical experiments, and no theory has been established yet. It is clear however that the two situations are not disconnected, the spectral width of an equivalent filter in the stochastic case being closely related to the ability of distinguishing between neighboring components in the deterministic case. A more precise approach is of course necessary, and it is under current investigation.

Appendix
Proof of Proposition 2

The proof is given only for the case where extrema are close to those of $x_1(t)$ since it is almost identical in the other case. The proof is based on a bijective function associating extrema of the sum signal to extrema of $x_1(t)$, as soon as $|af|$ is small enough. Let us first notice that the two functions being periodic and two times continuously differentiable, their derivatives and second derivatives are bounded: $|\partial_t x_i(t)| < M_i$, and $|\partial_t^2 x_i(t)| < M_i'$. Given these, we define

$$A = \min\left\{\frac{\eta}{M_2}, \frac{\epsilon}{M_2'}\right\}, \quad B = \max\left\{\frac{M_1}{\eta}, \frac{M_1'}{\epsilon}\right\}. \quad (14)$$

Let us define the sets $\{t_i\}$ and $\{t_j'\}$ as the locations of extrema in $x(t;a,f)$ and $x_1(t)$ respectively. Let us now consider an extremum of $x(t;a,f)$ at t_i, assuming $|af| < A$. Since $x'(t_i) = 0$, we can write

$$|\partial_t x_1(t_i)| = |-af\partial_t x_2(ft_i + \varphi)| < |a|fM_2 \leq \eta.$$

Let us then define the range $I_i =]b, c[$ as the largest open range containing t_i and such that for all $t \in I_i, |\partial_t x_1(t)| < \eta$. The latter is not empty since $\partial_t x_1(t)$ is continuous. Moreover, the boundaries b and c are finite because $x_1(t)$ being periodic and two times continuously differentiable, there are periodically locations where its second derivative is zero and therefore $|\partial_t x_1(t)| \geq \eta$. In addition, the continuity of $\partial_t x_1(t)$ allows us to write $|\partial_t x_1(b)| = |\partial_t x_1(c)| = \eta$ because I_i is the *largest*. Besides, for all $t \in I_i, |\partial_t^2 x_1(t)| > \epsilon$ which implies that $\partial_t^2 x_1(t)$ keeps the same sign over I_i. Assuming, for instance, that $\partial_t^2 x_1(t) > \epsilon$, then $\partial_t x_1(t)$ is nondecreasing over I_i and since $|\partial_t x_1(t_i)| < \eta$, the only possible values at the boundaries of I_i are $\partial_t x_1(b) = -\eta$ and $\partial_t x_1(c) = \eta$. Hence, there is an extremum t_j' of $x_1(t)$ in I_i that can be associated to t_i. Moreover, $\partial_t^2 x_1(t)$ being positive over I_i, there can only be one extremum of $x_1(t)$ in I_i, and it is a minimum. This allows us to define a function $\mathcal{F}$ that associates extrema of $x(t;a,f)$ to extrema of $x_1(t)$ according to the previous procedure. In addition, there is also a unique extremum of $x(t;a,f)$ in I_i because for all $t \in I_i$, $\partial_t^2 x(t;a,f) > \epsilon - af^2 M_2' > 0$. This implies that $\mathcal{F}$ is injective.

The next step is to prove that $\mathcal{F}$ is surjective. Let us now consider an extremum of $x_1(t)$ at t_j', assuming $|af| < A$. As before, we can define the largest range $I_j' =]b', c'[$ containing t_j' and such that for all $t \in I_j', |\partial_t x_1(t)| < \eta$, and if we assume for instance that t_j' is a minimum, then $\partial_t x_1(b') = -\eta$ and $\partial_t x_1(c') = \eta$. Let us show that there is an extremum of $x(t;a,f)$ in I_j' if $|af| < A$. At the boundaries, $\partial_t x(b') = -\eta + af\partial_t x_2(fb' + \varphi) < 0$ and $\partial_t x(c') = \eta + af\partial_t x_2(fc' + \varphi) > 0$ since $|M_2 af| < \eta$. Hence, there is an extremum t_i of $x(t;a,f)$ in I_j' and therefore the range I_j' corresponds to the range I_i as defined earlier for extremum t_i and thus $\mathcal{F}(t_i) = t_j'$, which proves that $\mathcal{F}$ is surjective. Since the lengths of the ranges I_i are all smaller than the period of $x_1(t)$, the identity between extrema rates of $x(t;a,f)$ and $x_1(t)$ follows from the existence of $\mathcal{F}$.

Finally, we can show that $\mathcal{F}(t_i) - t_i \to 0$ when $a \to 0$. To this aim, let us introduce $g_i(u)$, defined on $\partial_t x_1(I_i)$ as the inverse of the restriction of $\partial_t x_1(t)$ to I_i. $g_i(u)$ exists since $\partial_t^2 x_1(t) > \epsilon > 0$ on I_i. Thus, $t_i - \mathcal{F}(t_i) = g_i(\partial_t x_1(t_i)) - g_i(\partial_t x_1(\mathcal{F}(t_i)))$= $g_i(-af\partial_t x_2(ft_i + \varphi)) - g_i(0)$ which tends to zero when $a \to 0$ since $g_i(u)$ is continuous and $|af\partial_t x_2(ft_i + \varphi)| \leq |af|M_2 \to 0$.

Acknowledgment

The authors would like to thank P. Gonçalves (LIP-ENS Lyon) for many useful discussions.

References

[1] N. E. Huang, Z. Shen, S. R. Long, M. L. Wu, H. H. Shih, Q. Zheng, N. C. Yen, C. C. Tung, and H. H. Liu, "The empirical Mode Decomposition and Hilbert spectrum for nonlinear and non-stationary time series analysis," *Proc. Roy. Soc. London A*, vol. 454, pp. 903–995, 1998.

[2] J. R. N. Meeson, *Hilbert-Huang Transform and Its Applications*, N. E. Huang and S. S. P. Shen, Eds. Singapore: World Scientific, 2005.

[3] P. Flandrin and P. Gonçalves, "Empirical mode decompositions as a data-driven wavelet-like expansions," *Int. J. Wavelets, Multires., Inf. Process.*, vol. 2, no. 4, pp. 477–496, 2004.

[4] P. Flandrin, G. Rilling, and P. Gonçalves, "Empirical mode decomposition as a filter bank," *IEEE Signal Process. Lett.*, vol. 11, no. 2, pp. 112–114, 2004.

[5] R. C. Sharpley and V. Vatchev, "Analysis of the intrinsic mode functions," *Constr. Approx.*, vol. 24, pp. 17–47, 2006.

[6] K. T. Coughlin and K. K. Tung, "11-year solar cycle in the stratosphere extracted by the Empirical Mode Decomposition method," *Adv. Space Res.*, vol. 34, pp. 323–329, 2004.

[7] M. Chavez, C. Adam, V. Navarro, S. Boccaletti, and J. Martinerie, "On the intrinsic time scales involved in synchronization: A data-driven approach," *Chaos: An Interdisciplinary J. Nonlin. Sci.*, vol. 15, no. 2, pp. 023904–023904, 2005.

[8] A. Aïssa-El-Bey, K. Abed-Meraim, and Y. Grenier, "Underdetermined blind audio source separation using modal decomposition," *EURASIP J. Audio, Speech, Music Process.*, vol. 2007, pp. 15–15, 2007.

[9] G. Rilling, P. Flandrin, and P. Gonçalves, "On Empirical Mode Decomposition and its algorithms," presented at the IEEE-EURASIP Workshop Nonlinear Signal Image Processing (NSIP), Grado, Italy, Jun. 8–11, 2003.

[10] G. Rilling and P. Flandrin, "On the influence of sampling on the Empirical Mode Decomposition," presented at the IEEE Int. Conf. Acoustics, Speech, Signal Processing (ICASSP), Toulouse, France, 2006.

[11] M. Stevenson, M. Mesbah, and B. Boashash, "A sampling limit for the Empirical Mode Decomposition," in *Proc. Int. Symp. Signal Processing Its Applications (ISSPA)*, Sydney (A), 2005, pp. 647–650.

[12] J. R. N. Meeson, "HHT sifting and filtering," in *Hilbert-Huang Transform and Its Applications*, N. E. Huang and S. S. P. Shen, Eds. Singapore: World Scientific, 2005, pp. 75–105.

[13] M. Unser, "Splines: A perfect fit for signal processing," *IEEE Signal Process. Mag.*, vol. 16, no. 6, pp. 22–38, 1999.

[14] Z. Wu and N. E. Huang, "A study of the characteristics of white noise using the Empirical Mode Decomposition method," *Proc. Roy. Soc. London A*, vol. 460, pp. 1597–1611, 2004.

Gabriel Rilling studied physics at École Normale Supérieure de Lyon, France, where he received the "Professeur-Agrégé de Sciences Physiques" degree in 2003. He received the Master's degree in signal and image processing from the Université Cergy-Pontoise, France, in 2004. He is currently working towards the Ph.D. degree with the Signals, Systems and Physics Group, within the Physics Department at École Normale Supérieure de Lyon.

Patrick Flandrin (M'85–SM'01–F'02) received the Engineer degree from ICPI Lyon, France, in 1978 and the Doct.-Ing. and "Docteur d'État" degrees from INP Grenoble, France, in 1982 and 1987, respectively.

In 1982, he joined CNRS, where he is currently Research Director. Since 1991, he has been with the Signals, Systems and Physics Group, within the Physics Department at École Normale Supérieure de Lyon. In 1998, he spent one semester in Cambridge, U.K., as an invited long-term resident of the Isaac Newton Institute for Mathematical Sciences and, from 2002 to 2005, he was Director of the CNRS national cooperative structure "GdR ISIS." His research interests include mainly nonstationary signal processing (with emphasis on time-frequency and time-scale methods) and the study of self-similar stochastic processes. He has published many research papers in those areas, and he is the author of the book *Temps-Fréquence* (Paris, France: Hermès, 1993 and 1998), translated into English as *Time-Frequency/Time-Scale Analysis* (San Diego, CA: Academic, 1999).

Dr. Flandrin was awarded the Philip Morris Scientific Prize in Mathematics in 1991, the SPIE Wavelet Pioneer Award in 2001, and the Prix Michel Monpetit from the French Academy of Sciences in 2001. He was a co-Guest Editor of the Special Issue on Wavelets and Signal Processing of the IEEE TRANSACTIONS ON SIGNAL PROCESSING in 1993, the Technical Program Chairman of the 1994 IEEE Signal Processing Society International Symposium on Time-Frequency and Time-Scale Analysis and, since 2001, he has been the Program Chairman of the French GRETSI Symposium on Signal and Image Processing. He served as an Associate Editor for the IEEE TRANSACTIONS ON SIGNAL PROCESSING from 1990 to 1993, and he was a member of the Signal Processing Theory and Methods Technical Committee of the IEEE Signal Processing Society from 1993 to 2004.